

Coordinated Control and Energy Management of Distributed Generation Inverters in a AC/ DC Microgrid

Mr. Karneti Vamsi Krishna

M.Tech (Power Electronics)
Dhruva Institute and Technology
Nalgonda, Telangana 508252

Mr.V.Balu

Assistant Professor
Dhruva Institute and Technology
Nalgonda, Telangana 508252

Abstract

This paper presents a microgrid consisting of different distributed generation (DG) units that are connected to the distribution grid. An energy-management algorithm is implemented to coordinate the operations of the different DG units in the microgrid for grid-connected and islanded operations. The proposed microgrid consists of a photovoltaic (PV) array which functions as the primary generation unit of the microgrid and a proton-exchange membrane fuel cell to supplement the variability in the power generated by the PV array. A lithium-ion storage battery is incorporated into the microgrid to mitigate peak demands during grid-connected operation and to compensate for any shortage in the generated power during islanded operation. The control design for the DG inverters employs a new model predictive control algorithm which enables faster computational time for large power systems by optimizing the steady-state and the transient control problems separately. The design concept is verified through various test scenarios to demonstrate the operational capability of the proposed microgrid, and the obtained results are discussed.

I. INTRODUCTION

DUE TO increasing deployment of DGs in power systems, managing the power of different DGs and the grid has raised a major concern [1]–[3]. In this field, microgrids have become a widely accepted concept for the superior connection of DGs in power networks. Corresponding to the conventional power systems, ac microgrids have been established foremost and a variety of surveys have been reported particularly on

the subject of power sharing of parallel-connected sources [4]–[6]. Since the majority of renewable energy sources, generate dc power or need a dc link for grid connection and as a result of increasing modern dc loads, dc microgrids have recently emerged for their benefits in terms of efficiency, cost and system that can eliminate the dc-ac or ac-dc power conversion stages and their accompanied energy losses [7]–[10]. However, since the majority of the power grids are presently ac type, ac microgrids are still dominant and purely dc microgrids are not expected to emerge exclusively in power grids. Therefore, dc microgrids are prone to be developed in ac types even though in subordinate. Consequently, linking ac microgrids with dc microgrids and employing the profits of the both microgrids, has become interesting in recent studies [11]–[14].

Over the last decade, efficient and reliable communication and control technologies, coupled with an increase in smarter electrical facilities, such as electric vehicles and smart meters, have resulted in an increasing number of consumers participating in demand response management (DRM) [1]–[5]. The current research is also focused on achieving a smarter grid through demand-side management (DSM), increasing energy reserves and improving the power quality of the distribution system, such as harmonic compensation for nonlinear loads [5]–[8]. These new trends enable higher levels of penetration of renewable generation, such as wind and solar power into the grid. The integration of renewable sources can supplement the generation from the distribution grid. However, these renewable sources are intermittent in their generation and might compromise the reliability and

stability of the distribution network. As a result, energy-storage devices, such as batteries and ultra-capacitors, are required to compensate for the variability in the renewable sources. The incorporation of energy-storage devices is also critical for managing peak demands and variations in the load demand. In this paper, a microgrid consisting of a photovoltaic (PV) array, a proton-exchange membrane fuel cell (PEMFC), and a lithium-ion storage battery (SB) is proposed. The PEMFC is used as a backup generator unit to compensate for the power generated by the intermittent nature of the PV array. The SB is implemented for peak shaving during grid-connected operation, and to supply power for any shortage in generated power during islanded operation and to maintain the stability of the distribution network. An energy-management algorithm is designed for the microgrid to coordinate the sharing of power among different DG units. The proposed controller for the inverters of DG units is based on a newly developed model predictive control (MPC) algorithm, which optimizes the steady-state and the transient control problems separately. In this way, the computation time is greatly reduced.

In what follows, this paper provides a comprehensive solution for the operation of a microgrid which will simultaneously dispatch real and reactive power during both grid-connected and islanded operations, compensate for harmonics in the load currents, and perform peak shaving and load shedding under different operating conditions.

The idea is to merge the ac and dc microgrids through a bidirectional ac/dc converter and establishing a hybrid ac/dc microgrid in which ac or dc type energy sources and loads can flexibly integrate into the microgrids and power can smoothly flow between the two microgrids. Reference [11] proposes a hybrid ac/dc microgrid in which the renewable energy sources and storages are connected in a dc grid and supplying power to the main ac grid and local ac loads. A hybrid dc/ac microgrid configuration is proposed in [12], in which a dc power line along with an energy

conversion station are added to the conventional three-phase power distribution system for the integration of distributed domestic renewable sources. The main idea is to use the locally generated energy and reducing the power draw from the grid. Reference [13] proposes to combine a smart dc grid with the ac grid in order to suppress the dc bus voltage fluctuation using controllable loads and achieving the stabilization control of the ac grid using the grid-side converter interlinking the dc and ac microgrids. A hybrid microgrid composed of various kinds of renewable energy sources is considered in [14]. A coordinate control scheme is developed in order to manage the whole system in different operating conditions.

II. SYSTEM STRUCTURE AND OPERATION MODES

A simple hybrid ac/dc microgrid is shown in Fig. 1. It consists of an ac microgrid with conventional DG sources, a dc microgrid with two dc type sources and an IC links the two microgrids together. Each of these microgrids also includes their

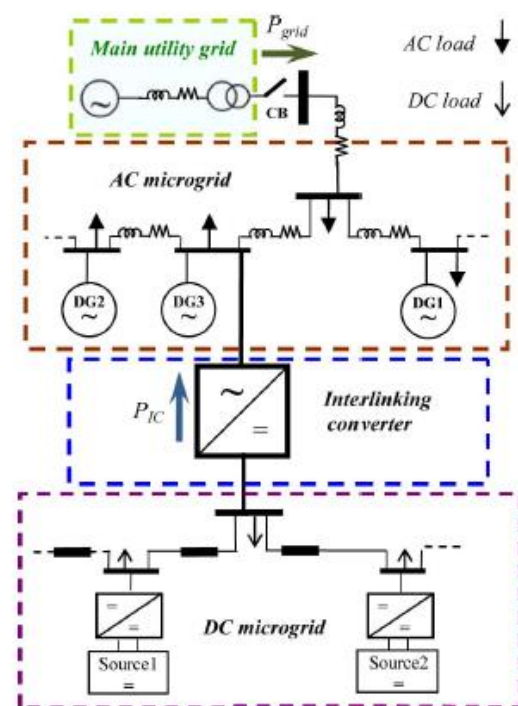


Fig.1. A typical hybrid ac/dc microgrid.

Individual loads. Besides, during normal grid operation the hybrid Microgrid is connected to the main utility grid through the ac microgrid. Basically, the microgrids are thought to operate in grid-connected or islanding modes [1]. In the grid-connected operation mode of the hybrid microgrid, the ac microgrid dynamics are governed directly by the main utility grid and the IC primarily regulates the dc microgrid voltage and controls the power balance, as well. In this operating condition the dc sources can generate a constant power or can operate in maximum power point for the renewable energy sources. In the islanding mode of operation, and during light loading of the dc part, the demanded power is shared among the dc sources using the P - V_{dc} droop characteristics. When over-loading happens in the dc microgrid, the interlinking converter will also participate in load sharing using the proposed ac-dc droop control. In the following, the performance of the hybrid ac/dc microgrid is described in either of these two modes.

A. Grid-Connected Mode

While the hybrid ac/dc microgrid is connected to the main utility grid, DG sources in the ac microgrid are expected to either generate a specified real/reactive power, or act as terminal voltage regulator with a specified amount of active power and variable reactive power [5]. On the other hand, the utility grid operates as slack bus to support the difference in the active/reactive power demand and to sustain the microgrid frequency. Similarly, in dc microgrid, DG sources would be controlled to generate a specified active power. However, the utility grid is still responsible for voltage support and power balance through the IC. According to Fig. 1 and neglecting the power losses, this mode can be described,

$$\text{dc microgrid : } P_{IC}^* = \sum_i P_{dc,i}^{load} + P_{dc}^{loss} - \sum_i P_{dc,i} \quad (1)$$

$$\text{ac microgrid : } P_{grid}^* = \sum_i P_{ac,i}^{load} + P_{ac}^{loss} + P_{IC}^* - \sum_i P_{ac,i} \quad (2)$$

In this mode the renewable energy sources in the microgrid can operate in maximum power point, energy storages can charge and non-renewable sources can be managed, e.g., for peak shaving purposes, loss reduction or economical goals [4]. In the ac microgrid, DGs could also generate a specified reactive power, regulate terminal voltage or may be used for power quality aims [21]. These power management studies have been studied in dc microgrids [7], [8] and it is not intended to be followed in this paper.

B. Islanding Mode

The more challenging situation is the islanding operation of the hybrid ac/dc microgrid. In the islanding mode, the total load demand should be shared and managed autonomously by the existing DGs in the both microgrids, which involves rapid and flexible active/reactive power control strategies to minimize the microgrid dynamics. A proper load shedding strategy is also required in case of deficiency in local generated power in order to maintain the system stability [7]. This paper adopts decentralized control strategies based on droop control to manage the power sharing among ac sources as well as dc sources, and between the ac and dc microgrid. Different operating states may occur during islanding operation of the hybrid microgrid. For the sake of appropriate performance of the hybrid ac/dc microgrid under different grid conditions, four main operating states are considered in the islanding mode, as follows:

Islanding state I: This operation state corresponds to the islanding operation of hybrid ac/dc microgrid during which power generation in ac microgrid and dc microgrid suffices their individual loads (light load condition). The generation units in each microgrid will regulate its power to meet the load. In this state, the IC halts transferring power and can just supply reactive power for the ac microgrid. This state is expressed by,

$$P_{IC}^* = P_{grid}^* = 0 \quad (3)$$

$$\text{dc microgrid : } \sum_i P_{dc,i}^{load} \leq \sum_i P_{dc,i} \quad (4)$$

$$\text{ac microgrid : } \sum_i P_{ac,i}^{load} \leq \sum_i P_{ac,i} \quad (5)$$

Islanding state II: This state represents the case where the generated power in ac microgrid is deficient for the ac load demand but there is surplus power in the dc microgrid. Therefore, the required power should be supplied by the dc sources through the IC. In this state we have,

$$\text{dc microgrid : } \sum_i P_{dc,i}^{load} < \sum_i P_{dc,i} \quad (6)$$

$$\text{ac microgrid : } \sum_i P_{ac,i}^{load} > \sum_i P_{ac,i} \quad (7)$$

$$P_{grid}^* = 0, P_{IC}^* = \sum_i P_{ac,i} - \sum_i P_{ac,i}^{load} - P_{ac}^{loss} \quad (8)$$

Islanding state III: This state is similar to state II, except that the power deficit occurs in the dc microgrid and the ac microgrid is in light load condition. Therefore, the ac microgrid supplies the required power for dc microgrid. In this case,

$$\text{dc microgrid : } \sum_i P_{dc,i}^{load} > \sum_i P_{dc,i} \quad (9)$$

$$\text{ac microgrid : } \sum_i P_{ac,i}^{load} < \sum_i P_{ac,i} \quad (10)$$

$$P_{grid}^* = 0, P_{IC}^* = \sum_i P_{dc,i} - \sum_i P_{dc,i}^{load} - P_{dc}^{loss} \quad (11)$$

Islanding state IV: This operation state relates to the case during which the load demand in both ac microgrid and dc microgrid are greater than the maximum available sources capacity (overload condition). In this state, the IC halts transferring power and a proper load shedding strategy must be run to stabilize the grids. This state is described by,

$$P_{IC}^* = P_{grid}^* = 0 \quad (12)$$

$$\text{dc microgrid : } \sum_i P_{dc,i}^{load} \geq \sum_i P_{dc,i} \quad (13)$$

$$\text{ac microgrid : } \sum_i P_{ac,i}^{load} \geq \sum_i P_{ac,i} \quad (14)$$

III. DROOP CONTROL STRATEGY FOR INDIVIDUAL MICROGRIDS

A. Control of DGS in the AC Microgrid

Power management based on droop control is currently well recognized in ac microgrids. Real power generation of a DG is specified based on frequency-droop (ω -P) characteristic [4]. Since there is no dominant source to enforce the base frequency in the islanded microgrid, the frequency of the microgrid varies by means of demanded power variations. The main idea of this control is to increase the active power generation of DGs when the system frequency decreases. Similarly, for reactive power management voltage-droop (V - P) is exploited. Reactive power generation of a DG is determined based on deviations in the bus voltage. Therefore, the DG source acts in response to the measured local voltage deviations caused by either the system or the local load. ω -P and V - P characteristics could be described mathematically by

$$P^{ref} = -\frac{1}{k_{ac}}(\omega^0 - \omega) + P^0 \quad (15)$$

$$Q^{ref} = -\frac{1}{k_q}(V^0 - V) + Q^0 \quad (16)$$

$$k_{p,ac} = -\frac{\omega^{max} - \omega^{min}}{P^{max}} \quad (17)$$

$$k_{q,ac} = -\frac{V^{max} - V^{min}}{Q^{max}} \quad (18)$$

By this power control method, during the grid-connected mode where the frequency of the system is fixed, real power generation of the DG is controlled by P^0 .

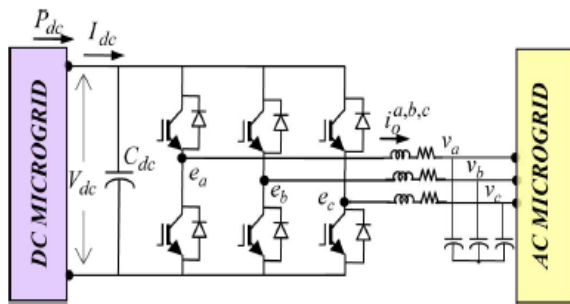


Fig.2. Configuration of the IC interfacing ac and dc microgrids.

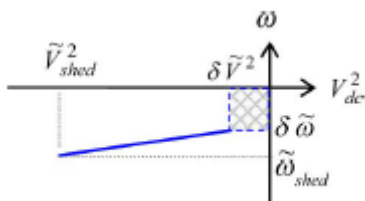


Fig.3. Proposed ac-dc droop characteristic.

B. Control of DGs in DC Microgrid

Alternatively, for the dc microgrid the dc voltage-droop ($V_{dc} - P$) control method is used for power sharing between DG sources in the microgrid. Typical $V_{dc} - P$ droop characteristics can be expressed by

$$P_{dc}^{ref} = -\frac{1}{k_{dc}}(V_{dc}^0 - V_{dc}) + P_{dc}^0 \quad (19)$$

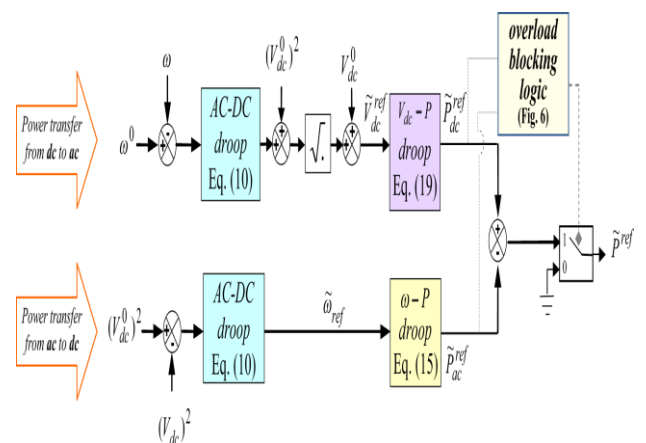
$$k_{p,dc} = -\frac{V_{dc}^{max} - V_{dc}^{min}}{P_{dc}^{max}} \quad (20)$$

IV. PROPOSED IC CONTROL FOR ISLANDING OPERATION

In addition to the power sharing strategies adopted for the standalone dc or ac microgrids, it is required to develop a proper control strategy for the IC to share the demanded power between these two microgrids. However, the power management for the IC control is different from the proposed strategies currently used for the energy sources in the standalone ac or dc microgrids. In contrast to the ac or dc microgrids, the IC is expected to manage a bidirectional flow of power between the ac and dc microgrids. In addition the IC

should cooperate in power sharing between the energy sources in both microgrids with dissimilar droop characteristics. This is due to the fact that at any instant the IC takes the role of supplier to one microgrid and at the same time acts as a load for the other microgrid. These challenging issues can be handled by exploiting a proper control strategy for the IC to transfer the required power between the microgrids. In order to eliminate fast communication links, a modified droop based control strategy is proposed to attain desirable performance. As discussed in the previous sections, during the islanding operation of the hybrid ac/dc micro grid different operating states might arise and the IC should recognize these states and manage the whole hybrid microgrid. The following decentralized control strategy is adopted for this purpose.

The power management should determine the amount of active power that the IC must transfer from one microgrid to the other. In order to provide the power reference command, the dc bus voltage of the IC and the frequency of the ac microgrid are utilized as input to the power management system. Considering Fig. 2, the electrical energy stored in the dc capacitor is,



$$W_{dc} = \frac{1}{2} C_{dc} V_{dc}^2 \quad (21)$$

Neglecting the switching losses in the converter $P_{dc} = P_{ac}$, the dynamics in the dc capacitor energy is the

difference of power transfer between ac and dc microgrids. Therefore,

$$\frac{d}{dt}W_{dc} = \frac{1}{2} C_{dc} \frac{d}{dt}(V_{dc}^2) = P_{dc} - P_{ac} = \Delta P. \quad (22)$$

On the other side, considering the ω -P characteristic in the ac microgrid,

$$\Delta \omega = \omega^0 - \omega = k_{\omega} \Delta P. \quad (23)$$

According to (22) and (23), using the forward Euler approximation with sampling period (T_c) [22] and assuming that the microgrid frequency is constant in this interval, a new droop characteristic for the IC called “ac-dc droop” is defined as,

$$(\omega_0 - \omega) = \bar{k}_{\omega} \left((V_{dc}^0)^2 - (V_{dc})^2 \right), \bar{k}_{\omega} = k_{\omega} \cdot \left(\frac{1}{2} \frac{C_{dc}}{T_s} \right). \quad (24)$$

The “ac-dc droop” characteristic is shown in Fig. 3. $\delta\omega$ and δV_{dc} are the dead zone bands for the allowable variation of angular frequency and dc voltage, respectively. Dead zone is utilized in the proposed “ac-dc droop” in order to prevent any power transfer during light load operation of individual micro grids. During such operation condition the generating units in each microgrid will regulate the generated power to supply the corresponding micro grid load using the relevant V_{dc} - P or ω - P droop characteristics. V_{dc}^{shed} and ω^{shed} are respectively the minimum dc voltage and ac microgrid frequency drop in dc and ac micro grids that the system is supposed to undergo load shedding.

Furthermore, since the IC is not the mere frequency or dc voltage controller in the hybrid ac/dc microgrid, it is necessary to participate in power sharing between ac and dc sources. To implement this scheme, the output of the ac-dc droop is fed to the V_{dc} - P and ω - P droops of the IC. It is necessary to mention that since positive sign for power transfer in the IC is considered to be from dc to ac, the power for V_{dc} - P droop should be regarded with negative sign. Finally, according to \bar{V}_{dc}^{ref} and $\bar{\omega}^{ref}$ the amount of power to be transferred via the IC is determined by the two reference power calculated through these two loops. A schematic block

diagram of the proposed power management strategy for the IC is depicted in Fig. 4. The impact of the proposed droop control for the IC on the power sharing of sources in each microgrid is illustrated within two load increase scenarios in each microgrid,

1) In the first scenario it is assumed that the dc microgrid is near overloading and there is excess power in the ac microgrid. Upon increasing the load in the dc microgrid, the dc voltage will accordingly decrease. If the voltage drop is beyond δV , referring to the proposed ac-dc droop (Fig. 3) this voltage deviation produces a new reference angular frequency $\bar{\omega}^{ref}$. This $\bar{\omega}^{ref}$ will then determine the reference power for the IC power controller using the conventional ω - P droop. This is the amount of power to be transferred from ac to dc microgrid. Therefore, the IC treats as a source for the dc microgrid and partly restores the voltage of the dc microgrid. On the other hand, the IC takes the roll of a load for the ac microgrid and increases the power generation of the ac sources.

2) The other scenario happens when the ac microgrid is near overloading. When the ac load increases again, causes the frequency to decrease below $\delta\omega$. Referring to the proposed ac-dc droop a new reference voltage (\bar{V}_{dc}^{ref}) is presented. Finally, by using the droop the required power to be transferred to the V_{dc} - P dc microgrid is determined. Therefore, according to these two scenarios whenever the load increases in one of the microgrids, the “ac-dc droop” characteristic relates the ac and dc microgrids using the dc link performance and the equivalent frequency droop characteristic of the ac microgrid which is determined by,

$$\Delta P = k_{\omega} \Delta \omega, k_{\omega} = \left(\frac{1}{R_1} + \frac{1}{R_2} + \dots + \frac{1}{R_n} \right) + D \quad (25)$$

Where R_1, \dots, R_n are droop coefficient of ac sources D and is the load-damping constant of the ac microgrid. Using this droop characteristic it is possible to relate the different droops of ac and dc microgrid and consequently share the power in the whole microgrid.

By this power management strategy the response of IC indifferent islanding states is as follows:

Islanding state I: Throughout this state, $\Delta\omega < \delta\omega$ and $\Delta V_{dc}^2 < \delta V^2$ therefore the output of “ac-dc droop” is

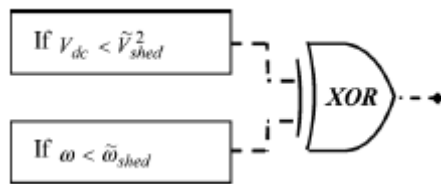


Fig.5. Overload blocking logic for real power controller of the IC.

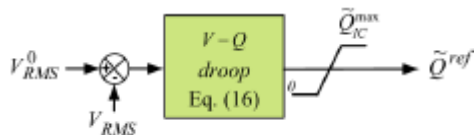


Fig.6. Reactive power controller for the IC.

$\bar{V}_{dc}^{ref} = V_{dc}^0$ For dc micro grid and $\bar{\omega}^{ref} = \omega_0$ for ac microgrid. Consequently, $\bar{P}^{ref} = 0$ and IC transfers no power.

Islanding state II: In this state $\Delta V_{dc}^2 < \delta V^2$ but $\Delta\omega < \delta\omega$. Therefore, $\bar{P}^{ref} = -\bar{P}_{dc}^{ref}$ and IC supplies power to the ac microgrid.

Islanding state III: In this state $\Delta\omega < \delta\omega$ but $\Delta V_{dc}^2 > \delta V^2$ therefore, and IC supplies power to the dc microgrid.

Islanding state IV: During this state, $\omega < \omega_{shed}$ and $\Delta V_{dc}^2 < \delta V^2_{shed}$. In order to block the IC for any power transfer, an overload blocking logic shown in Fig. 5, is added at the output the proposed droop control in which by using an “EXCLUSIVE OR(XOR)” logic, whenever both microgrids enter

overloading the IC is blocked and no power will transfer.

The reactive power control of the IC is more straightforward since there is no reactive power in dc microgrid and the IC is designated to play as a voltage support in droop-control mode to share the reactive power with other DGs in ac microgrid. The reactive power sharing is based on the conventional droop shown in Fig. 6, the local RMS voltage is measured and using the droop, the V-Q reactive power reference is determined. Since the active power transfer is the prime task of the IC, a dynamic reactive power limit is added to the control block to consider the capacity limit of the IC. The reactive limit is defined as,

$$\bar{Q}_{IC}^{max} = \sqrt{(S_{IC}^{max})^2 - P_{IC}^2} \tag{26}$$

Finally, a current control scheme [23] is utilized in IC control for tracking the reference active/reactive power calculated by the power management system.

V. MODELING AND SMALL SIGNAL STABILITY ANALYSIS

Section IV describes the proposed droop method for the IC in the hybrid AC/DC microgrid. This section investigates a small signal analysis for the hybrid microgrid to analyze the stability of the system. In order to reduce system equations and for the better analysis of the proposed droop controller, the dc sources and their individual droops are aggregated to form one combined dc source. This is also done for ac sources, dc and ac loads as well. Therefore the hybrid microgrid shown in Fig. 1 is simplified from the perspective of IC, as shown in Fig. 7. Furthermore, as discussed in Section II, different scenarios can be considered for the operation of the hybrid microgrid, but for the stability analysis only the worst case condition is considered which is the islanding states II and III defined in Section II.

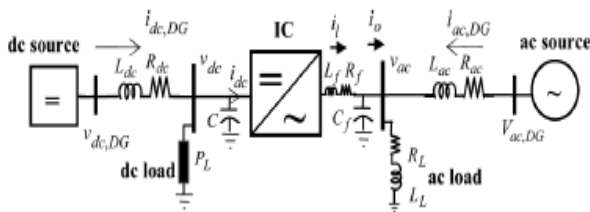


Fig.7. Simplified equivalent model of the hybrid microgrid.

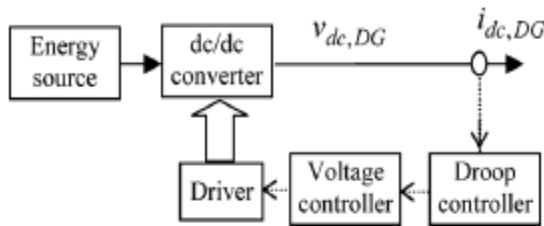


Fig.8. Block diagram of the dc source.

A. DC Micro grid Modeling

The dc microgrid comprised of sources, loads and the dc network. Components modeling are discussed in the following subsections.

1) DC Source Modeling:

The block diagram of a dc source is shown in Fig. 8. By measuring the output current of the dc source and using the droop controller, the reference voltage value for the voltage controller of the dc/dc converter is determined. Since the voltage controller are much faster than the droop controller [25] and in order to reduce the system equations, the fast dynamics are neglected and the dc/dc converter is assumed to be a controllable voltage source. This means that the voltage controller can exactly follow the reference voltage and consequently the output voltage is equal to its reference value. The droop equation for the dc source is,

$$v_{dc,DG} = \frac{1}{R_{dc}} i_{dc,DG} + v_{dc,DG}^0 \quad (27)$$

Linearizing (26) by using small-signal approximation leadsto,

The represents the small-signal perturbation of the corresponding parameter.

2) DC Load Model:

The majority of loads in the dc microgrid utilize power electronic converters for grid connection since these converters are generally tightly regulated; these loads behave as a constant power load (CPL) [26]. Therefore, the CPL load model is considered for stability analysis. As shown in [26], the small signal model of CPL can be expressed by a negative resistance, as given by

$$\hat{i}_{L,dc} = g_L \cdot \hat{v}_{L,dc} \quad (29)$$

$$g_L = -\frac{P_L}{V_{L,dc}^2}$$

3) DC Network Model:

The dc network is equivalently modeled as a series combination of resistance and reactance as shown in Fig. 7. The network equation can be represented as follows,

$$\hat{v}_{dc} = L_{dc} \frac{d\hat{i}_{dc,DG}}{dt} + R_{dc} \hat{i}_{dc,DG} \quad (30)$$

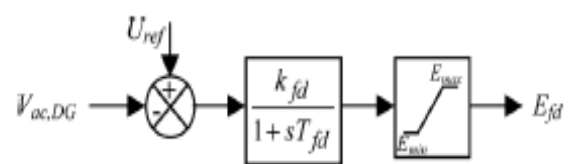


Fig.9. Excitation system model of synchronous generator.

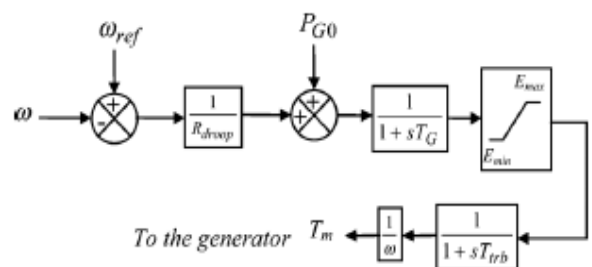


Fig.10. Governor and turbine model of synchronous generator.

B. Ac Micro grid Modeling

Similar to dc micro grid, the ac micro grid is also consists of acsources, ac loads and the ac network, as shown in Fig. 7. The aggregated ac source is a two-pole, three-phase synchronous machine, equipped with excitation and governor systems. Detailed small signal modeling of the synchronous machine is fully considered in [27] and for the sake of brevity this is not presented here. A first-order excitation system is used for terminal voltage control, as shown in Fig. 9. The equation of this system is,

$$\dot{E}_{fd} = \frac{k_{fd}}{T_{fd}}(U_{ref} - E_t) - E_{fd} \tag{31}$$

Two first-order governor and turbine are adapted to control the frequency, as shown in Fig. 10.

The small signal state space model of the load and the ac network are,

$$\frac{d\hat{i}_{L,ac}^d}{dt} = -\frac{R_L}{L_L}\hat{i}_{L,ac}^d + \omega\hat{i}_{L,ac}^q + \frac{1}{L_L}\hat{v}_{ac}^d \tag{32}$$

$$\frac{d\hat{i}_{L,ac}^q}{dt} = -\frac{R_L}{L_L}\hat{i}_{L,ac}^q - \omega\hat{i}_{L,ac}^d + \frac{1}{L_L}\hat{v}_{ac}^q \tag{33}$$

$$\begin{aligned} \frac{d\hat{i}_{ac,DG}^d}{dt} = & -\frac{R_{ac}}{L_{ac}}\hat{i}_{ac,DG}^d + \omega\hat{i}_{ac,DG}^q \\ & + \frac{1}{L_{ac}}(\hat{v}_{ac}^d - \hat{v}_{ac,DG}^d) \end{aligned} \tag{34}$$

$$\begin{aligned} \frac{d\hat{i}_{ac,DG}^q}{dt} = & -\frac{R_{ac}}{L_{ac}}\hat{i}_{ac,DG}^q - \omega\hat{i}_{ac,DG}^d \\ & + \frac{1}{L_{ac}}(\hat{v}_{ac}^q - \hat{v}_{ac,DG}^q). \end{aligned} \tag{35}$$

C. IC Modeling

Fig. 11 shows the control block diagram of the IC in *d-q* reference frame. The real power reference is determined according to the proposed droop shown in Fig. 4. The active power control loop generates the reference current i^*d using PI controller. The current control loop measures the output currents and

control the converter to follow the reference value using PI controller.

The droop characteristics for active power shown in Fig. 4 can be expressed by,

$$(\omega_0 - \omega) = \bar{k}_\omega \left((V_{dc,DG}^0)^2 - (v_{dc,DG})^2 \right) \tag{36}$$

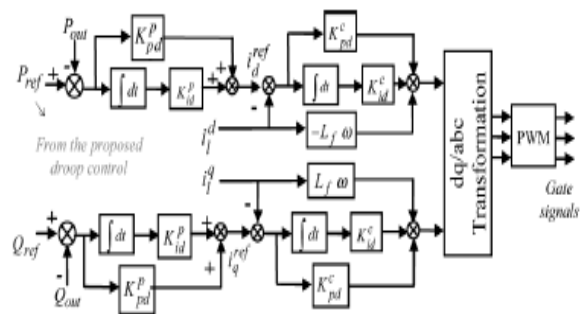


Fig.11. Control block diagram of the IC.

$$P_{ac}^{ref} = k_{ac}(\omega_{ref} - \omega) \tag{37}$$

$$P_{dc}^{ref} = k_{dc}(V_{dc,DG}^{ref} - v_{dc,DG}). \tag{38}$$

Combining (35) and (36), the reference power for the ac microgrid is,

$$P_{ac}^{ref} = k_{ac} \left[\left(\frac{1}{\bar{k}_\omega} (v_{dc,DG}^2 - V_{dc,DG}^0)^2 + \omega_0 \right) - \omega \right]. \tag{39}$$

The linearized model of the proposed droop for the ac microgrid can be obtained as,

$$\begin{aligned} \hat{P}_{ac}^{ref} = & \alpha_{ac} \hat{v}_{dc,DG} - k_{ac} \hat{\omega} \\ \alpha_{ac} = & 2 \frac{k_{ac}}{\bar{k}_\omega} V_{dc,DG} \end{aligned} \tag{40}$$

Where V_{dc} is the dc-bus voltage at the operating point. Similarly, the linearized reference power for the dc microgrid can be expressed by,

$$\hat{P}_{dc}^{ref} = \alpha_{dc} \hat{v}_{dc,DG} - k_{dc} \hat{\omega}$$

$$\alpha_{dc} = -\frac{k_{dc} \bar{k}_{\omega}}{2\sqrt{\omega_0}} V_{dc,DG} \quad (41)$$

A conventional PLL [28] is used for estimating the system angular frequency, ω . The linearized model of the PLL is represented by,

$$\hat{\omega} = -K_{pll} K_{p\omega} \hat{\omega} - K_{pll} K_{i\omega} m_q \hat{v}_{ac}^q - K_{pll} K_{i\omega} m_d \hat{v}_{ac}^d \quad (42)$$

The parameters are defined in [28].

The linearized model of real power controller derived from Fig. 11 is [4]

$$\hat{\phi}_{id} = \hat{P}_{ref} - \hat{P}_{out} \quad (43)$$

$$\hat{v}_d^{ref} = K_{id}^p \hat{\phi}_{id} + K_{pd}^p (\hat{P}_{ref} - \hat{P}_{out}) \quad (44)$$

\hat{P}_{out} is represented by the linearized equation of the instantaneous real power in the d - q frame as,

Finally, the reference voltage for the PWM switching is followed by the current controller according to the reference current. The corresponding small-signal state space equation of the current controller is,

$$\hat{\phi}_{vd} = \hat{v}_d^{ref} - \hat{v}_l^d \quad (46)$$

$$\hat{v}_d^{ref} = K_{pd}^c (\hat{v}_d^{ref} - \hat{v}_l^d) + K_{id}^c \hat{\phi} - \hat{\omega} L_f \hat{v}_l^d \quad (47)$$

Since the dc bus voltage in the IC is not fixed, the switching process should also be considered for stability analysis. There

TABLE I
POWER FLOW IN EACH OPERATING CASE

	Case I	Case II
Ac source generation (kW)	645	624
Dc source generation (kW)	440	461
IC power transfer (kW)	-55 (ac to dc)	-33 (ac to dc)
Dc load (kW)	490	490
Ac load (kW)	580	580
k_{ω} ((rad/s)/kW)	12	20

TABLE II
TWO DOMINATING OPERATING MODES

	Case I	Case II
Mode 1	-0.074 ± j8.75	-0.054 ± j8.68
Mode 2	-1.36 ± j 3.2	-1.43 ± j 3.1

Fore, the converter and its output filter small signal model can be represented by [29],

$$\frac{d\hat{i}_o^d}{dt} = -\frac{R_f}{L_f} \hat{i}_o^d + \omega \hat{i}_o^q + \frac{1}{L_f} \hat{v}_{ac}^d - V_{dc} \hat{d}_d - \hat{v}_{dc} D_d \quad (48)$$

$$\frac{d\hat{i}_o^q}{dt} = -\frac{R_f}{L_f} \hat{i}_o^q - \omega \hat{i}_o^d + \frac{1}{L_f} \hat{v}_{ac}^q - V_{dc} \hat{d}_q - \hat{v}_{dc} D_q \quad (49)$$

$$C \frac{d\hat{v}_{dc}}{dt} = \frac{3}{2} (\hat{d}_d I_l^d + \hat{d}_q I_l^q + D_d \hat{i}_l^d + D_q \hat{i}_l^q) - \hat{i}_{dc} \quad (50)$$

$$\frac{d\hat{v}_{ac}^d}{dt} = \omega \hat{v}_{ac}^q + \frac{1}{C_f} \hat{i}_l^d - \frac{1}{C_f} \hat{i}_o^d \quad (51)$$

$$\frac{d\hat{v}_{ac}^q}{dt} = -\omega \hat{v}_{ac}^d + \frac{1}{C_f} \hat{i}_l^q - \frac{1}{C_f} \hat{i}_o^q \quad (52)$$

The small signal model of the hybrid ac/dc microgrid is developed by combining the state-space representation of each subsystem transferred to a global reference frame and the state-space model of the dc microgrid.

D. Small Signal Analysis

The linearized model of the hybrid microgrid is used to study the small signal dynamics of the microgrid during autonomous mode of operation. Based on the system model and corresponding parameters, the two dominating modes are:

Mode 1: Electromechanical mode of ac source which is selected as a gas-fired turbine-generator

Mode 2: Related to the droop gain of the IC which is the function of k_{dc} , k_{ac} , k_{ω} .

The dominant modes are identified for two operating cases shown in Table I. The first case corresponds to the power transfer from the ac to dc microgrid with $k_{\omega} = 12$ (this corresponds to the value for the proportional power sharing between the sources [4]) and the second relates to the power transfer with $k_{\omega} = 20$. The corresponding modes are shown in Table II. It is found that by increasing the ac-dc droop gain, the amount of power participation for the ac source decreases which increases the ac source damping (dominating mode). The same result can be deduced for the power transfer from dc to ac, in which increasing the ac-dc droop gain results in the greater participation of dc sources in the power sharing and increases the dominating mode damping.

Different operating scenarios, configuration of loads and generation are considered in the simulations in order to validate the performance of the proposed power management method in controlling the IC in the hybrid ac/dc microgrid and sharing the power between the ac and dc microgrids.

A. Case 1

In this case, the hybrid ac/dc microgrid is supposed to be connected to the main utility grid. At first, dc sources generate a fixed power, a portion of the demanded load is supplied by the local sources in dc microgrid and the insufficient power is provided through the IC. At $t=1s$, a large portion of the dc load switches off and the dc power generation is more than the load demand. The IC moves to the inverting mode and feeds the surplus power to the ac grid. Similarly, at $t=2s$ dc load increases and approximately matches the generated dc power. The IC power, dc load and the generated power of the dc sources along with dc-bus voltage are shown in Fig. 12. It can be concluded that the IC can smoothly balance the power inside the dc microgrid during grid-connected mode. Throughout this control strategy, the dc sources are allowed to follow the energy management strategies and considering the economic facts straightforwardly [30].

B. Case 2

This case simulates the hybrid ac/dc microgrid operation in transition from grid-connected mode to islanding mode. Before islanding occurs, the dc microgrid is in light load condition and feeds the surplus power to the ac grid. At $t=1s$ the microgrid is disconnected from the main grid, and the islanding event is detected by the IC at $t=1.06s$. A 60 ms delay is assumed for typical islanding detection methods [31]. The IC control strategy is changed from the grid-connected to the proposed control strategy for islanding control of the hybrid ac/dc microgrid. The demanded ac load is greater than the generated power in the ac microgrid and causes the frequency drop. In order to balance the power, the IC controller shares the surplus power in the dc microgrid with the ac sources in the ac microgrid. During the islanding

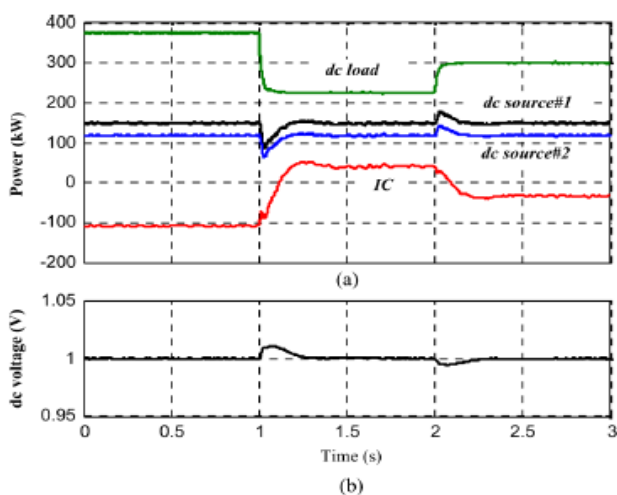


Fig.12. Simulation results for Case 1.

VI. CASE STUDIES AND SIMULATION RESULTS

In order to validate the proposed power management control, a hybrid ac/dc microgrid is simulated in PSCAD/EMTDC using detailed switching model for the converters. Considering the schematic diagram of Fig. 1, the ac microgrid includes two gas-fired DG units with synchronous generators, excitation and governor control systems. Furthermore, the dc microgrid contains two dispatchable dc sources. System parameters are presented in Appendix.

operation at $t=2$ s the ac load is increased further and this causes the IC to transfer more power from the dc to ac microgrid. Simulation results are shown in Fig. 13. The increase in the ac load leads to frequency drop in the ac microgrid. The IC as well as the ac sources detects the frequency drop and by using the proposed droop characteristic the amount of power to be transferred to the ac microgrid is determined and shared between the dc sources. Simulation results are also summarized in Table III for the steady state generation conditions. It can be seen that the load is proportionally shared between the ac and dc sources. A small sharing error in the power sharing is due to the different voltage level that is sensed by the sources in the dc microgrid. Results show that this control strategy can maintain the power balance by sharing the total load demand between the existing ac and dc sources and prevents any frequency drift and need for load shedding during the time that the demanded power is less than the sum of the ac and dc sources rating.

C. Case 3

Similar to case 2, this case also deals with the situation of transition from the grid-connected into the islanding mode but, despite case 2 in this case the ac microgrid is operated in light load condition and the dc microgrid is over loaded. At $t=1$ s the microgrid is disconnected from the main grid, and since the dc load power is greater than the rated power of the dc sources, causes dc voltage-drop. In order to balance the power, the IC controller shares the surplus power in the ac microgrid with the dc sources in the dc microgrid. During the islanding operation at $t=2$ s the dc load is increased further and this causes the IC to transfer more power from the ac to the dc microgrid. Simulation results are shown in Fig. 14. The increase in the dc load is detected by the dc sources first and results in voltage drop. The IC also perceives this voltage drop and by using the proposed droop characteristic the amount of power to be transferred to the dc microgrid is determined and shared between the ac sources. Simulation results are also summarized in Table IV for the steady state generation conditions. It can be seen that the load is proportionally shared

between the ac and dc sources. Small sharing error in the power sharing is due to the different voltage level that is sensed by the sources in the dc microgrid. It can be realized that the proposed control strategy can accurately manage the power imbalance by sharing the demanded power between the sources in both ac and dc microgrids and avoids any instability in ac and dc microgrids.

D. Case 4

In order to evaluate the performance of the proposed control strategy in different load profiles during the islanding operation, the islanded hybrid ac/dc microgrid is simulated in case 4. The two microgrids are initially operating in light load condition;

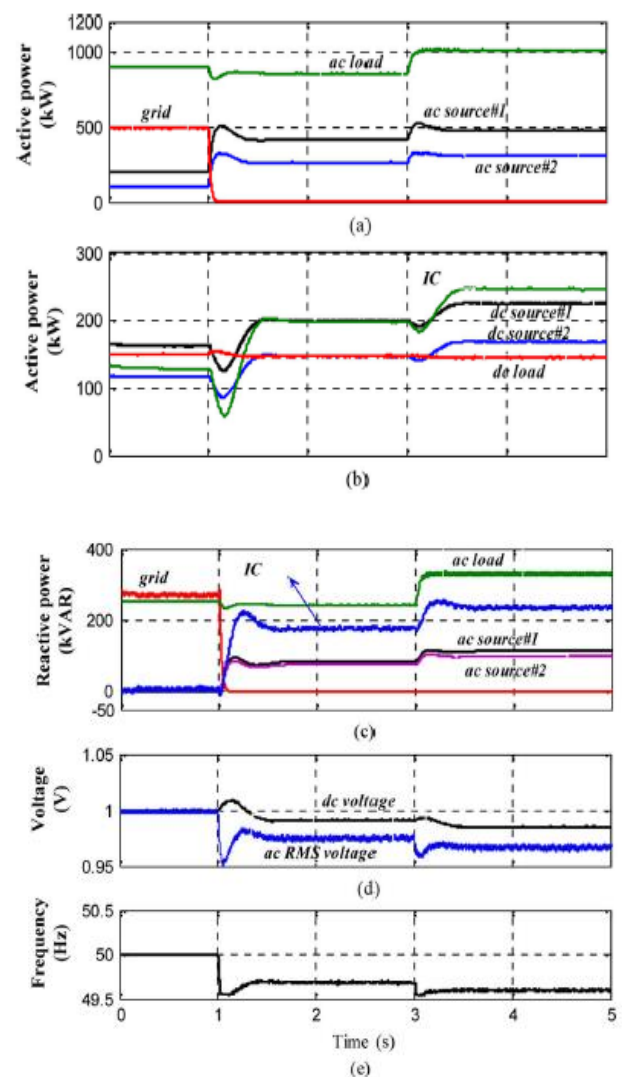


Fig.13. Simulation results for Case 2.

TABLE III
STEADY-STATE OPERATING CONDITIONS OF SOURCES IN CASE 2

	t= 1-3 sec	t= 3-5 sec
Total load (kW)	1000	1150
ac source #1 (kW)	390	450
ac source #2 (kW)	250	280
dc source #1 (kW)	210	255
dc source #2 (kW)	170	185

this means that the load power in both ac microgrid and dc microgrid are less than the total rating of individual sources. According to the control strategy, when the microgrids are operated in light load condition the IC transfers no power. At $t=1$ s a load increase happens in the ac microgrid in which the power demand is greater than available ac generation, the IC detects the frequency drop and calculates the required power to be transferred from dc to ac microgrid (P_{dc}^{req}) and shares this power demand between sources. Then at $t=2$ s again the load decreases and the ac microgrid enters the light load condition. After that at $t=3$ s dc load is increased and the IC detects the voltage drop and calculates the required power to be fed to dc microgrid (P_{ac}^{req}) and shares this power demand between sources. Simulation results are shown in Fig. 15. And the steady state results are

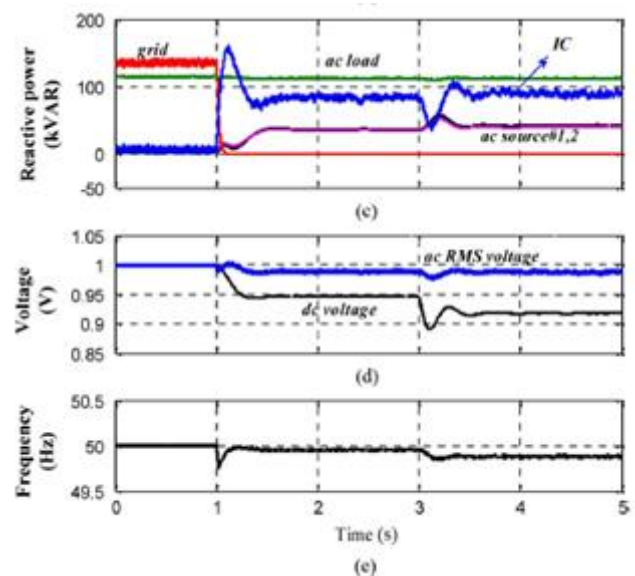


Fig.14. Simulation results for Case 3.

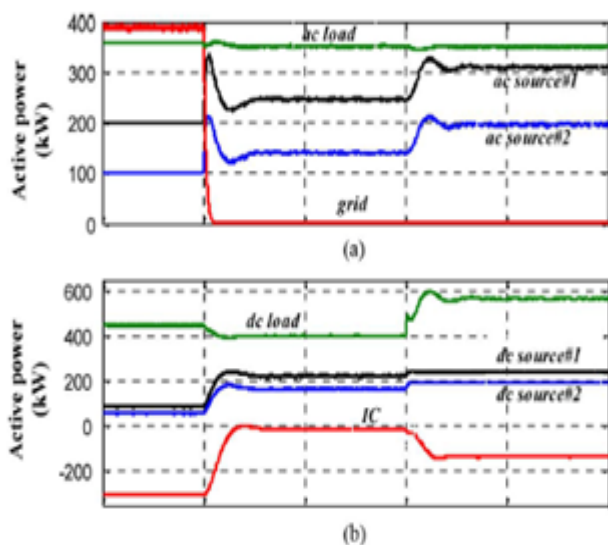
TABLE IV
STEADY-STATE OPERATING CONDITIONS OF SOURCES IN CASE 3

	t= 1-3 sec	t= 3-5 sec
Total load (kW)	750	920
ac source #1 (kW)	230	320
ac source #2 (kW)	140	200
dc source #1 (kW)	215	220
dc source #2 (kW)	170	200

Summarized in Table V. It can be realized that the IC can reasonably manage the power sharing and avoids any instability during the autonomous operation of the hybrid microgrid.

E. Case 5

Case 5 simulates the performance of the IC facing over load condition on both ac and dc microgrids. Both microgrids are primarily operating in light load condition. At $t=1$ s the load power is increased in the dc microgrid and causes overloading of the microgrid in which the IC feeds the required power. At $t=2$ s the ac load is also increased and makes the ac microgrid over loaded. While both microgrids are over loaded, the IC transfers no power and each microgrid is responsible



for the power management. Due to power deficiency in both micro-

and over load blocking logic in this study case. It is necessary to mention that if the overload blocking is not used, it makes the interconnection of the power management control between the ac and dc microgrids, which causes power swing between ac and dc.

F. Case 6

In this case the participation of the DC microgrid on the system frequency is studied by varying droop gain of the IC

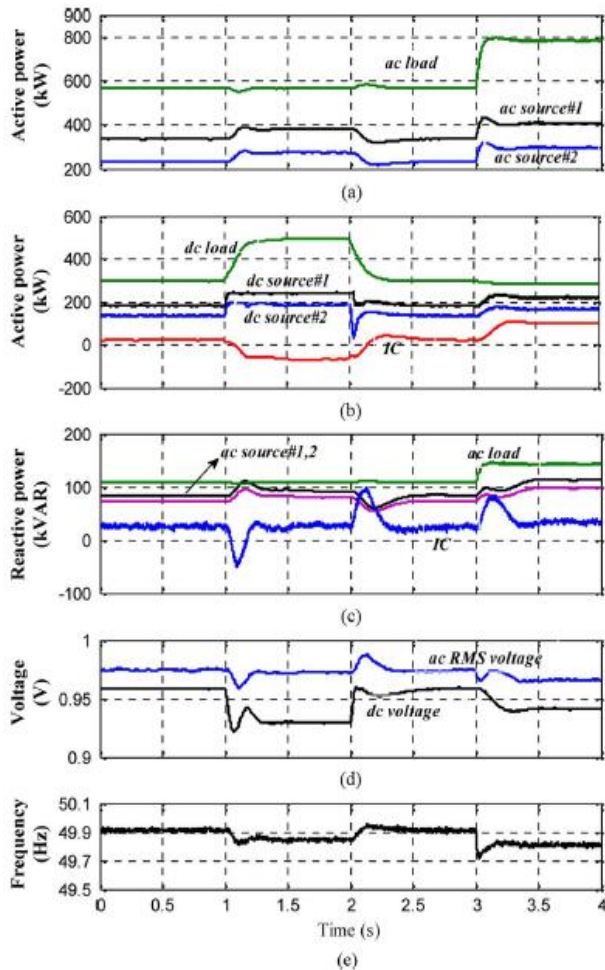


Fig.15. Simulation results for Case 4.

TABLE V
STEADY-STATE OPERATING CONDITIONS OF SOURCES IN CASE 4

	t=0-1 sec	t=1-2 sec	t=2-3 sec	t=3-4 sec
Total load (kW)	865	1060	865	1070
ac source #1 (kW)	330	390	340	400
ac source #2 (kW)	215	265	215	280
dc source #1 (kW)	190	245	185	230
dc source #2 (kW)	150	190	145	175

Grids, dc voltage drops below allowable voltage range (0.9 p.u) and activates the dc load shedding system. On the other hand, the ac frequency also drops and a portion of ac load is shed to stabilize the ac microgrid. Fig. 16 shows the performance of the hybrid microgrid

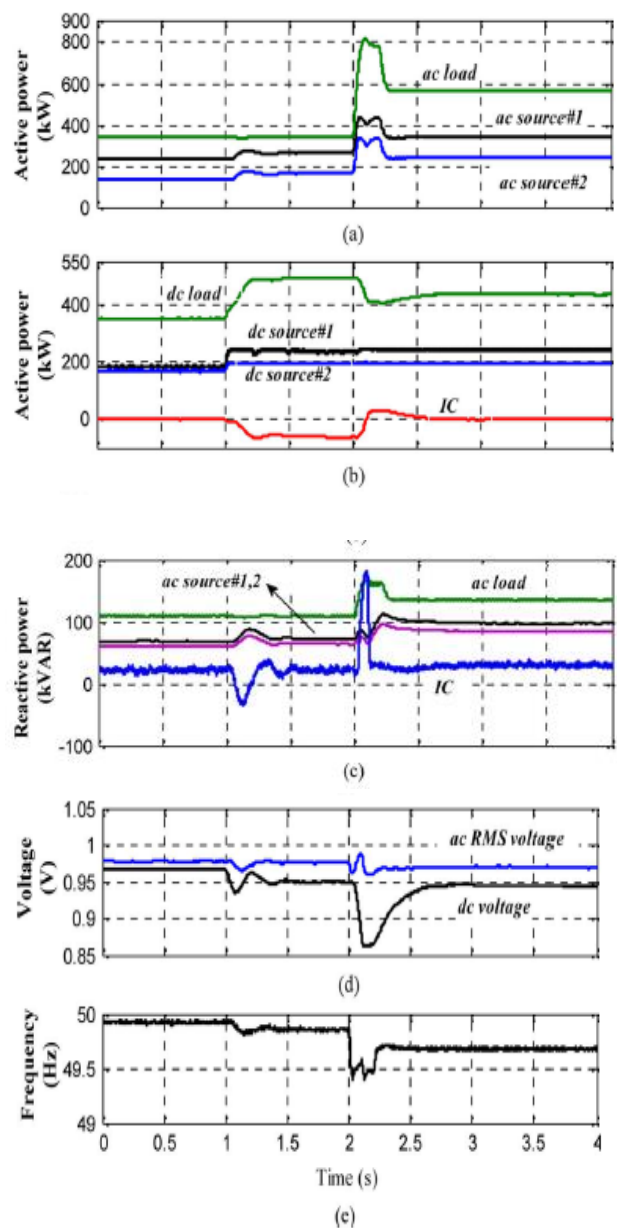


Fig.16. Simulation results for Case 5.

TABLE VI

PARTICIPATION OF THE DC MICROGRID ON THE SYSTEM FREQUENCY

k_{ω}	8	12	20
Steady-state frequency (Hz)	49.05	49.42	49.73

(k_{ω}) For a similar load change in the ac microgrid. Simulation results are shown in Table VI. When k_{ω} increases the participation of dc microgrid on the ac microgrid increases which results in smaller steady-state frequency deviation.

VII. CONCLUSION

This paper proposes a decentralized control strategy based on the two-stage modified droop method for the control of the IC interfacing dc and ac microgrids. This hybrid microgrid architecture prepares an infrastructure for flexible connection of different ac or dc loads and sources to the grid. By measuring the ac microgrid frequency and the dc microgrid voltage and using proposed droop characteristic, the power management strategy provides the power reference for the IC control to share the power demand between the existing power sources in both ac and dc microgrids. Using the proposed droop method, the IC is able to perform power sharing between the two microgrids in the transition from grid-connected to islanding mode as well as during the islanding operation. This makes it possible to decrease the required power conversion stages and hence the system cost and efficiency. The performance of the proposed control strategy considering different operating states is demonstrated through time-domain simulation of a hybrid ac/dc microgrid in the PSCAD/EMTDC software. A more sophisticated control strategy for power sharing control of several interconnected ac and dc microgrids can be extended from the result of this work, which is under investigation by the authors for the future study.

TABLE VIII
DC SOURCES PARAMETERS

	dc source 1	dc source 2
Rating (nominal)	300 (kW)	250 (kW)
R_{dc}	0.0013 (A/V)	0.0011 (A/V)

TABLE IX
IC PARAMETERS.

	dc source 1
Rating (nominal)	300 (kVA)
DC voltage	1500 (V)
DC capacitance	5000 (μ F)
Filter capacitance	2500 (μ F)
Filter inductance	100 (μ H)
K_{dc}	2 (kW/V)
K_{ac}	11.9 (kW/(rad/s))
K_{ω}	11.45 (kW/(rad/s))

REFERENCES

- [1] F. Katiraei, M. R. Iravani, A. L. Dimeas, and N. D. Hatziargyriou, "Microgrids management: control and operation aspects of microgrids," IEEE Power Energy Mag., vol. 6, no. 3, pp. 54–65, May/Jun. 2008.
- [2] R. H. Lasseter and P. Paigi, "Microgrid: A conceptual solution," in Proc. IEEE-PESC'04, 2004, pp. 4285–4290.
- [3] H. Nikkhajoei and R. H. Lasseter, "Distributed generation interface to the cert microgrid," IEEE Trans. Power Del., vol. 24, no. 3, pp. 1598–1608, Jul. 2009.
- [4] F. Katiraei and M. R. Iravani, "Power management strategies for a microgrid with multiple distributed generation units," IEEE Trans. Power Syst., vol. 21, no. 4, pp. 1821–1831, Nov. 2006.

- [5] C. K. Sao and P. W. Lehn, "Control and power management of converterfed microgrids," *IEEE Trans. Power Syst.*, vol. 23, no. 3, pp.1088–1098, Aug. 2008.
- [6] I.-Y. Chung, W. Liu, D. A. Cartes, E. G. Collins, Jr, and S. Moon, "Control methods of inverter-interfaced distributed generators in a microgridssystem," *IEEE Trans. Ind. App.*, vol. 46, no. 3, pp. 1078–1088, May/June. 2010.
- [7] N. Eghtedarpour and E. Farjah, "Control strategy for distributed integrationof photovoltaic and energy storage systems in dc microgrids," *J. Renewable Energy*, vol. 45, pp. 96–110, Sep. 2012.
- [8] L. Xu and D. Chen, "Control and operation of a DC microgrid withvariable generation and energy storage," *IEEE Trans. Power Del.*, vol.26, no. 4, pp. 2513–2522, Oct. 2011.
- [9] M. E. Baran and N. R. Mahajan, "DC distribution for industrial systems-opportunities and challenges," *IEEE Trans. Ind. App.*, vol. 39,no. 6, pp. 1596–1601, Nov./Dec. 2003.
- [10] N. Eghtedarpour and E. Farjah, "Distributed charge/discharge controlof energy storages in a renewable-energy-based DC microgrid," *IETRenew. Power Gen.*, vol. 8, no. 1, pp. 45–57, Jan. 2014.
- [11] D. Bo, Y. Li, Z. Zheng, and L. Xu, "Control strategies ofmicrogridwithhybrid DC and AC buses," in *Proc. 14th Eur. Conf. Power Electron.Appl. (EPE 2011)*, pp. 1–8.
- [12] A. Karabiber, C. Keles, A. Kaygusuz, and B. B. Alagoz, "An approachfor the integration of renewable distributed generation in hybrid DC/ACmicrogrids," *J. Renewable Energy*, vol. 52, pp. 251–259, Apr. 2013.
- [13] K. Kurohane, T. Senjyu, A. Yona, N. Urasaki, and T. Funabashi, "Ahybrid smart AC/DC power system," *IEEE Trans. Smart Grid*, vol. 1,no. 2, pp. 199–204, Sep. 2010.
- [14] X. Liu, P. Wang, and P. C. Loh, "Ahybrid AC/DC microgrid and its coordinationcontrol," *IEEE Trans. Smart Grid*, vol. 2, no. 2, pp. 278–286, 2011.
- [15] M. N. Ambia, A. Al-Durra, and S. M. Mueeen, "Centralized powercontrol strategy for AC-DC hybrid microgrid system using multi-convertercheme," in *Proc. IECON 2011—37th Annu. Conf. IEEE Ind.Electron. Soc.*, Nov. 2011, pp. 843–848.
- [16] J. M. Guerrero, J. C. Vasquez, J. Matas, L. G. Vicuña, andM. Castilla, "Hierarchical control of droop-controlled AC and DC microgrids-ageneral approach toward standardization," *IEEE Trans. Ind. Electron.*, vol. 58, no. 1, pp. 158–166, Jan. 2011.
- [17] P.C.Loh, D. Li, Y. K. Chai, and F. Blaabjerg, "Autonomous operationof hybrid microgrid with AC and DC subgrids," *IEEE Trans. PowerElectron*, vol. 28, no. 5, pp. 2214–2223, May 2013.
- [18] C. Jin, P. C. Loh, P. Wang, Y. Mill, and F. Blaabjerg, "Autonomousoperation of hybrid AC-DC microgrids," in *Proc. IEEE ICSET, Kandy, Sri Lanka*, Dec. 6–9, 2010.
- [19] P. C. Loh, D. Li, Y. K. Chai, and F. Blaabjerg, "Autonomous control ofinterlinking converter with energy storage in hybridAC-DCmicrogrid," *IEEE Trans. Ind. Appl.*, vol. 49, no. 3, pp. 1374–1382, May/June. 2013.
- [20] P.C. Loh, D. Li, Y. K. Chai, and F. Blaabjerg, "HybridAC-DCmicrogridswith energy storages and progressive energy flow tuning," *IEEE Tran. Power Electron*. Vol. 28, no. 4, pp. 1533–1543, Apr. 2013.
- [21] J. C. Vasquez, R. A. Mastromauro, J. M. Guerrero, and M. Liserre, "Voltage support provided by a droop-controlled multifunctional inverter," *IEEE Trans. Ind. Electron.*, vol. 56, no. 11, pp. 4510–4519, Nov. 2009.

[22] C. Du, E. Agneholm, and G. Olsson, "Comparison of different frequency controllers for a VSC-HVDC supplied system," *IEEE Trans. Power Del.*, vol. 23, no. 4, pp. 2224–2232, Oct. 2008.

[23] A. Yazdani and R. Iravani, *Voltage-Sourced Converters in Power Systems: Modeling, Control, and Applications*. Hoboken, NJ, USA: Wiley, 2010.

[24] P. Kundur, *Power System Stability and Control*. New York: Mc-Graw-Hill, 1994.

[25] S. Anand and B. G. Fernandes, "Reduced-order model and stability analysis of low-voltage dc microgrid," *IEEE Trans. Ind. Electron.*, vol. 60, no. 11, pp. 5040–5049, Nov. 2013.

[26] A. M. Rahimi and A. Emadi, "An analytical investigation of DC/DC power electronic converters with constant power loads in vehicular power systems," *IEEE Trans. Veh. Tech.*, vol. 58, no. 6, pp. 2689–2702, Jul. 2009.

[27] P. C. Krause, *Analysis of Electric Machinery and Drive Systems*. Piscataway, NJ, USA: IEEE Press, 2002.

[28] F. Katiraei, M. R. Iravani, and P. W. Lehn, "Small-signal dynamic model of a micro-grid including conventional and electronically-interfaced distributed resources," *Proc. Inst. Elect. Eng., Gen., Transm., Distrib.*, vol. 1, no. 3, pp. 369–378, 2007.

[29] V. Blasko and V. Kaura, "A new mathematical model and control of a three-phase AC-DC voltage source converter," *IEEE Trans. Power Electron.*, vol. 12, no. 1, pp. 116–123, Jan. 1997.

[30] A. K. Basu, S. P. Chowdhury, S. Chowdhury, and S. Paul, "Microgrids: Energy management by strategic deployment of DERs-A comprehensive survey," *Renewable Sustain. Energy Rev.*, vol. 15, no. 9, pp. 4348–4356, Dec. 2011.

[31] H. Karimi, H. Nikkhajoei, and R. Iravani, "Control of an electronically coupled distributed resource unit subsequent to an islanding event," *IEEE Trans. Power Del.*, vol. 23, no. 1, pp. 493–501, Jan. 2008.



Mr. KARNETI VAMSI KRISHNA. He is pursuing M.Tech (Power Electronics) at Dhruva Institute of Engineering and Technology. Completed his B.Tech (EEE) from Narasaraopeta Institute of Technology, Narasaraopet, A.P.



Mr. V. BALU he received M.E (Power Systems) from University College of Engineering, Osmania University, Hyderabad in 2008 A.P. Graduated from JNTU University, Hyderabad in the year 2002. Presently he is working as Assistant Professor in Dhruva Institute of Engineering & Technology, Hyderabad in the Department of Electrical & Electronics Engineering. He had total 9 years of experience in teaching. His fields of interest include power quality and Power Systems Optimization.